Introduction to Plasma Physics

INTRODUCTION TO PLASMA PHYSICS

Robert J Goldston
and
Paul H Rutherford

Plasma Physics Laboratory
Princeton University

CRC Press
Taylor & Francis Group
Boca Raton London New York

CRC Press is an imprint of the
Taylor & Francis Group, an **informa** business

CRC Press
Taylor & Francis Group
6000 Broken Sound Parkway NW, Suite 300
Boca Raton, FL 33487-2742

First issued in hardback 2018

ISBN-13: 978-0-7503-0183-1 (pbk)
ISBN-13: 978-1-138-45831-4 (hbk)

Library of Congress catalog number- 95-37117

The software that originally came with this book is now available for download on the Web site.

Library of Congress Cataloging-in-Publication Data

Catalog record is available from the Library of Congress

Visit the Taylor & Francis Web site at
http://www.taylorandfrancis.com

and the CRC Press Web site at
http://www.crcpress.com

Dedicated to

Ruth Berger Goldston

and

Audrey Rutherford

Contents

Preface

Plasmas occur pervasively in nature: indeed, most of the known matter in the Universe is in the ionized state, and many naturally occurring plasmas, such as the surface regions of the Sun, interstellar gas clouds and the Earth's magnetosphere, exhibit distinctively plasma-dynamical phenomena arising from the effects of electric and magnetic forces. The science of plasma physics was developed both to provide an understanding of these naturally occurring plasmas and in furtherance of the quest for controlled nuclear fusion. Plasma science has now been used in a number of other practical applications, such as the etching of advanced semiconductor chips and the development of compact x-ray lasers. Many of the conceptual tools developed in the course of fundamental research on the plasma state, such as the theory of Hamiltonian chaos, have found wide application outside the plasma field.

Research on controlled thermonuclear fusion has long been a world-wide enterprise. Major experimental facilities in Europe, Japan and the United States, as well as smaller facilities elsewhere including Russia, are making remarkable progress toward the realization of fusion conditions in a confined plasma. The use, for the first time, of a deuterium–tritium plasma in the tokamak experimental fusion device at the Princeton Plasma Physics Laboratory has recently produced slightly in excess of ten megawatts of fusion power, albeit for less than a second. In 1992, an agreement was signed by the European Union, Japan, the Russian Federation and the United States of America to undertake jointly the engineering design of an experimental reactor to demonstrate the practical feasibility of fusion power.

This book is based on a one-semester course offered at Princeton University to advanced undergraduates majoring in physics, astrophysics or engineering physics. If the more advanced material, identified by an asterisk after the Chapter heading or Section heading, is included then the book would also be suitable as an introductory text for graduate students entering the field of plasma physics.

We have attempted to cover all of the basic concepts of plasma physics with reasonable rigor but without striving for complete generality—especially where this would result in excessive algebraic complexity. Although single-particle,

fluid and kinetic approaches are introduced independently, we emphasize the interconnections between different descriptions of plasma behavior; particular phenomena which illustrate these interconnections are highlighted. Indeed, a unifying theme of our book is the attempt at a deeper understanding of the underlying physics through the presentation of multiple perspectives on the same physical effects. Although there is some discussion of weakly ionized gases, such as are used in plasma etching or occur naturally in the Earth's ionosphere, our emphasis is on fully ionized plasmas, such as those encountered in many astrophysical settings and employed in research on controlled thermonuclear fusion, the field in which both of us work. The physical issues we address are, however, applicable to a wide range of plasma phenomena. We have included problems for the student, which range in difficulty from fairly straightforward to quite challenging; most of the problems have been used as homework in our course.

Standard international (SI) units are employed throughout the book, except that temperatures appearing in formulae are in units of energy (i.e. joules) to avoid repeated writing of Boltzmann's constant; for practical applications, temperatures are generally stated in electron-volts (eV). Appendices A and C allow the reader to convert from SI units to other units in common use.

The student should be well-prepared in electromagnetic theory, including Maxwell's equations, which are provided in SI units in Appendix B. The student should also have some knowledge of thermodynamics and statistical mechanics, including the Maxwell–Boltzmann distribution. Preparation in mathematics must have included vectors and vector calculus, including the Gauss and Stokes theorems, some familiarity with tensors or at least the underlying linear algebra, and complex analysis including contour integration. Appendix D contains all of the vector formulae that are used, while Appendix E gives expressions for the relevant differential operators in various coordinate systems. Higher transcendental functions, such as Bessel functions, are avoided. Suggestions for further reading are given in Appendix F.

In addition to the regular problems, which are to be found in all chapters, we have provided a disk containing two graphics programs, which allow the student to experiment visually with mathematical models of quite complex plasma phenomena and which form the basis for some homework problems and for optional semester-long student projects. These programs are provided in both Macintosh[1] and IBM PC-compatible format. In the first of these two computer programs, the reader is introduced to the relatively advanced topic of area-preserving maps and Hamiltonian chaos; these topics, which form another of the underlying themes of the book, reappear later in our discussions both of the magnetic islands caused by resistive tearing modes and of the nonlinear

[1] Macintosh is a registered trademark of Apple Computer, Inc.

phase of electron plasma waves.

We are deeply indebted to Janet Hergenhan, who prepared the manuscript in LaTeX format, patiently resetting draft after draft as we reworked our arguments and clarified our presentations. We would also like to thank Greg Czechowicz, who has drawn many of the figures, John Wright, who produced the IBM-PC versions of our programs, and Keith Voss, who served for three years as our 'grader', working all of the problems used in the course and offering numerous excellent suggestions on the course material.

We are grateful to Maureen Clarke and, more recently, James Revill of Institute of Physics Publishing, who have suffered patiently through our many delays in producing a completed manuscript.

Our own research in plasma physics and controlled fusion has been supported by the United States Department of Energy, Contract No. DE-AC02-76-CHO-3073.

Robert J Goldston
Paul H Rutherford
Princeton, 1995

Introduction

After an initial Chapter, which introduces plasmas, both in the laboratory and in nature, and derives the defining characteristics of the plasma state, this book is divided into six 'Units'. In Unit 1, the plasma is considered as an assemblage of charged particles, each moving independently in prescribed electromagnetic fields. After deriving all of the main features of the particle orbits, the topic of 'adiabatic' invariants is introduced, as well as the conditions for 'non-adiabaticity', illustrating the latter by means of the modern dynamical concepts of mappings and the onset of stochasticity. In Unit 2, the fluid model of a plasma is introduced, in which the electromagnetic fields are required to be self-consistent with the currents and charges in the plasma. Particular attention is given to demonstrating the equivalence of the particle and fluid approaches. In Unit 3, after an initial Chapter which describes the most important atomic processes that occur in a plasma, the effects of Coulomb collisions are treated in some detail. In Unit 4, the topic of small-amplitude waves is covered in both the 'cold' and 'warm' plasma approximations. The treatment of waves in the low-frequency branch of the spectrum leads naturally, in Unit 5, to an analysis of three of the most important instabilities in non-spatially-uniform configurations: the Rayleigh–Taylor (flute), resistive tearing, and drift-wave instabilities. In Unit 6, the kinetic treatment of 'hot' plasma phenomena is introduced, from which the Landau treatment of wave–particle interactions and associated instabilities is derived; this is then extended to the non-uniform plasma in the drift-kinetic approximation.

Chapter 1

Introduction to plasmas

1.1 WHAT IS A PLASMA?

First and foremost, a plasma is an ionized gas. When a solid is heated sufficiently that the thermal motion of the atoms breaks the crystal lattice structure apart, usually a liquid is formed. When a liquid is heated enough that atoms vaporize off the surface faster than they recondense, a gas is formed. When a gas is heated enough that the atoms collide with each other and knock their electrons off in the process, a plasma is formed: the so-called 'fourth state of matter'. Exactly when the transition between a 'very weakly ionized gas' and a 'plasma' occurs is largely a matter of nomenclature. The important point is that an ionized gas has unique properties. In most materials the dynamics of motion are determined by forces between near-neighbor regions of the material. In a plasma, charge separation between ions and electrons gives rise to electric fields, and charged-particle flows give rise to currents and magnetic fields. These fields result in 'action at a distance', and a range of phenomena of startling complexity, of considerable practical utility and sometimes of great beauty.

Irving Langmuir, the Nobel laureate who pioneered the scientific study of ionized gases, gave this new state of matter the name 'plasma'. In greek $\pi\lambda\alpha\sigma\mu\alpha$ means 'moldable substance', or 'jelly', and indeed the mercury arc plasmas with which he worked tended to diffuse throughout their glass vacuum chambers, filling them like jelly in a mold[1].

[1] We also like to imagine that Langmuir listened to the blues. Maybe he was thinking of the song 'Must be Jelly 'cause Jam don't Shake Like That', recorded by J Chalmers MacGregor and Sonny Skylar. This song was popular in the late 1920s, when Langmuir, Tonks and Mott-Smith were studying oscillations in plasmas.

1.2 HOW ARE PLASMAS MADE?

A plasma is not usually made simply by heating up a container of gas. The problem is that for the most part a container cannot be as hot as a plasma needs to be in order to be ionized—or the container itself would vaporize and become plasma as well.

Typically, in the laboratory, a small amount of gas is heated and ionized by driving an electric current through it, or by shining radio waves into it. Either the thermal capacity of the container is used to keep it from getting hot enough to melt—let alone ionize—during a short heating pulse, or the container is actively cooled (for example with water) for longer-pulse operation. Generally, these means of plasma formation give energy to free electrons in the plasma directly, and then electron–atom collisions liberate more electrons, and the process cascades until the desired degree of ionization is achieved. Sometimes the electrons end up quite a bit hotter than the ions, since the electrons carry the electrical current or absorb the radio waves.

1.3 WHAT ARE PLASMAS USED FOR?

There are all sorts of uses for plasmas. To give one example, if we want to make a short-wavelength laser we need to generate a population inversion in highly excited atomic states. Generally, gas lasers are 'pumped' into their lasing states by driving an electric current through the gas, and using electron–atom collisions to excite the atoms. X-ray lasers depend on collisional excitation of more energetic states of partially ionized atoms in a plasma. Sometimes a magnetic field is used to hold the plasma together long enough to create the highly ionized states.

A whole field of 'plasma chemistry' exists where the chemical processes that can be accessed through highly excited atomic states are exploited. Plasma etching and deposition in semiconductor technology is a very important related enterprise. Plasmas used for these purposes are sometimes called 'process plasmas'.

Perhaps the most exciting application of plasmas such as the ones we will be studying is the production of power from thermonuclear fusion. A deuterium ion and a tritium ion which collide with energy in the range of tens of keV have a significant probability of fusing, and producing an alpha particle (helium nucleus) and a neutron, with 17.6 MeV of excess energy (alpha particle $\sim$ 3.5 MeV, neutron $\sim$ 14.1 MeV). A promising way to access this energy is to produce a plasma with a density in the range $10^{20}\,\mathrm{m}^{-3}$ and average particle energies of tens of keV. The characteristic time for the thermal energy contained within such a plasma to escape to the surrounding material surfaces must exceed about five seconds, in order that the power produced in alpha particles can

sustain the temperature of the plasma. This is not a simple requirement to meet, since electrons within a fusion plasma travel at velocities of $\sim 10^8\,\mathrm{m\,s^{-1}}$, while a fusion device must have a characteristic size of $\sim 2\,\mathrm{m}$, in order to be an economic power source. We will learn how magnetic fields are used to contain a hot plasma.

The goal of producing a plentiful and environmentally benign energy source is still decades away, but at the present writing fusion power levels of 2–10 MW have been produced in deuterium–tritium plasmas with temperatures of 20–40 keV and energy confinement times of 0.25–1 s. This compares with power levels in the 10 mW range that were produced in deuterium plasmas with temperatures of ~ 1 keV and energy confinement times of ~ 5 ms in the early 1970s. It is the quest for a limitless energy source from controlled thermonuclear fusion which has been the strongest impetus driving the development of the physics of hot plasmas.

1.4 ELECTRON CURRENT FLOW IN A VACUUM TUBE

Let us look more closely now at how a plasma is made with a dc electric current. Consider a vacuum tube (not filled with gas), with a simple planar electrode structure, as shown in Figure 1.1. Imagine that the cathode is sufficiently heated that copious electrons are boiling off of its surface, and (in the absence of an applied electric field) returning again. Now imagine we apply a potential to draw some of the electrons to the anode. First, let us look at the equation of motion for the electrons:

$$m_e \frac{\mathrm{d}\mathbf{v}_e}{\mathrm{d}t} = -e\mathbf{E} = e\nabla\phi \tag{1.1}$$

where m_e is the electron mass (9.1×10^{-31} kg), $\mathbf{v}_e$ is the vector electron velocity ($\mathrm{m\,s^{-1}}$), e is the unit charge (1.6×10^{-19} C), $\mathbf{E}$ is the vector electric field ($\mathrm{V\,m^{-1}}$), and ϕ is the electrical potential (V). To derive energy conservation, we take the dot product of both sides with $\mathbf{v}_e$:

$$m_e \mathbf{v}_e \cdot \frac{\mathrm{d}\mathbf{v}_e}{\mathrm{d}t} = \tfrac{1}{2} m_e \frac{\mathrm{d}v_e^2}{\mathrm{d}t} = e\mathbf{v}_e \cdot \nabla\phi. \tag{1.2}$$

The total (or convective) derivative, moving with the particle, is defined by

$$\frac{\mathrm{d}}{\mathrm{d}t} \equiv \frac{\partial}{\partial t} + \mathbf{v}_e \cdot \nabla. \tag{1.3}$$

Thus the total (convective) time derivative of the electric potential, ϕ, moving with the electron, can be viewed as being made up of a part having to do with the potential changing in time at a fixed location (the partial derivative, $\partial/\partial t$),

plus a part having to do with the changing location at which we must evaluate ϕ. Since in this case we are considering a *steady-state* electric field, the partial (non-convective) time derivatives are zero. Thus we have

$$\frac{\mathrm{d}}{\mathrm{d}t}\left(\frac{m_e v_e^2}{2}\right) = \frac{\mathrm{d}}{\mathrm{d}t}(e\phi) \tag{1.4}$$

or, moving along the trajectory of an electron,

$$\frac{m_e v_e^2}{2} - e\phi = \text{constant}. \tag{1.5}$$

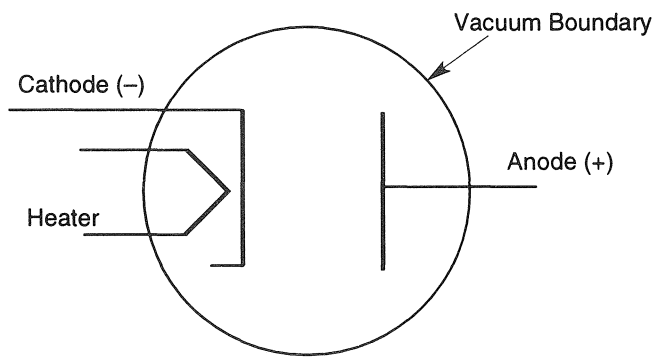

Figure 1.1. Vacuum-tube geometry for a hot-cathode Child–Langmuir calculation.

Equation (1.5) gives us some important information about the electron velocity in the inter-electrode space of our vacuum tube. If for simplicity we assign $\phi = 0$ to the cathode (since the offset to ϕ can be chosen arbitrarily), and negligibly small energy to the random 'boiling' energy of the electrons near the cathode, then the constant on the right-hand side of equation (1.5) can be taken to be zero, and

$$v_e \approx \left(\frac{2e\phi}{m_e}\right)^{1/2}. \tag{1.6}$$

Note that, in this case, v_e is not a random thermal velocity, but rather a directed flow of the electrons—the individual velocities of the electrons and the average velocity of the electron 'fluid' are the same. As a consequence of this 'fluid' velocity of the electrons, there is a net current density $\mathbf{j}$ (amperes/meter^2) $\equiv -n_e e \mathbf{v}_e$ flowing between the two electrodes, where n_e is the number density of electrons—the electron 'count' per cubic meter. In order to understand this current, it is helpful to think of a differential cube, as shown in Figure 1.2, with edges of length $\mathrm{d}l$, volume $(\mathrm{d}l)^3$, and total electron count in the cube of

$n_e(dl)^3$. Imagine that the electron velocity is directed so that the contents are flowing out of one face of the cube (see Figure 1.2). If the fluid is moving at v_e (meters/second), the cube of electrons is emptied out across that face in time dl/v_e seconds. Thus, $en_e(dl)^3$ units of charge cross $(dl)^2$ square meters of surface in dl/v_e seconds—the current density is thus $en_e(dl)^3/[(dl/v_e)(dl)^2] = n_e e v_e$ (coulombs/second · meter^2, i.e. amperes/meter^2), as we stated above.

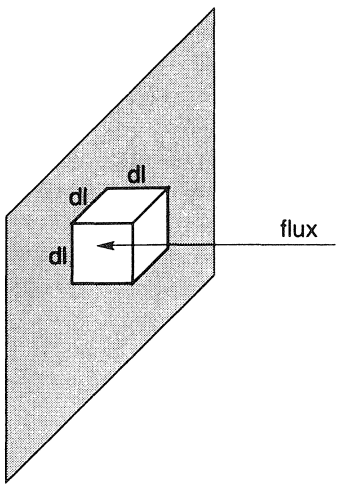

Figure 1.2. Geometry for interpreting $\mathbf{j} = -n_e e \mathbf{v}_e$.

If we now consider the integral of this particle current over the surface area of a given volume, we have the total flow of particles out of the volume per second, and so the time derivative of the total number of particles in a given volume of our vacuum tube is given by

$$\frac{\partial N_e}{\partial t} = -\int n_e \mathbf{v}_e \cdot d\mathbf{S} = 0 \tag{1.7}$$

where N_e is the total number of particles in a volume, and $d\mathbf{S}$ is an element of area of its surface. Here we assume that there are no sources or sinks of electrons within the volume; by setting the result to zero we are positing a steady-state condition. By Gauss's theorem, this can be expressed in differential notation as

$$\frac{\partial n_e}{\partial t} = -\nabla \cdot (n_e \mathbf{v}_e) = 0. \tag{1.8}$$

Poisson's equation is of course

$$\nabla \cdot (\epsilon_0 \nabla \phi) = e n_e \tag{1.9}$$

where ϵ_0, the permittivity of free space, is $8.85 \times 10^{-12}\,\mathrm{C\,V^{-1}\,m^{-1}}$.

The complete set of equations we need to solve in order to understand the current flow in our evacuated tube is then made up of equations (1.6), (1.8), and (1.9). Before we go on to solve these equations, we can immediately see a useful overall scaling relation. If we imagine taking any valid solution of this set of equations, and scaling ϕ by a factor α everywhere, then equation (1.9) tells us that n_e must scale by the same factor α. Equation (1.6) says that v_e must scale everywhere by $\alpha^{1/2}$. Equation (1.8) is also satisfied by this result, since $n_e v_e$ is scaled everywhere equally by $\alpha^{3/2}$. In the conditions we have been describing, with plenty of electrons boiling off the cathode (so there is no limit to the source of electrons at the boundary of our problem), the total current in the tube scales as $\phi^{3/2}$. This is called the Child–Langmuir law.

The condition we are considering is called space-charge-limited current flow. If too few electrons are available from the cathode, the current can fall below the Child–Langmuir law. It is then called emission-limited current flow. For the specific case of planar electrodes, with a gap smaller than the typical electrode dimensions, we can approximate the situation using one-dimensional versions of equations (1.8) and (1.9):

$$-n_e e v_e = j = \text{constant} \tag{1.10}$$

and

$$\frac{\mathrm{d}}{\mathrm{d}x}\left(\epsilon_0 \frac{\mathrm{d}\phi}{\mathrm{d}x}\right) = e n_e. \tag{1.11}$$

Substituting equation (1.6), we have

$$\epsilon_0 \frac{\mathrm{d}^2\phi}{\mathrm{d}x^2} = e n_e = -j/v_e = -j\left(\frac{m_e}{2e\phi}\right)^{1/2} \tag{1.12}$$

We can find a solution to this nonlinear equation simply by assuming that $\phi \propto x^\beta$, where β is some constant power. Looking at the powers of x that occur on each side, we come to the conclusion that

$$\beta - 2 = -\beta/2 \qquad \text{or} \qquad \beta = 4/3. \tag{1.13}$$

So now we can assume that $\phi = Ax^{4/3}$ which, when substituted into equation (1.12), gives

$$\epsilon_0 A(4/3)(1/3) = -j\left(\frac{m_e}{2eA}\right)^{1/2} \tag{1.14}$$

or

$$\phi(x) = \left(\frac{-9j}{4\epsilon_0}\right)^{2/3}\left(\frac{m_e}{2e}\right)^{1/3} x^{4/3}. \tag{1.15}$$

This solution is appropriate for our conditions, where we have taken the potential to be zero at the cathode, and since so many electrons are 'boiling' around the

cathode, we have assumed that negligible electric field strength is required to extract electrons from this region. Thus we have chosen the solution that has $d\phi/dx = 0$ where $\phi = 0$, i.e. at $x = 0$. Let us now make the last step of deriving the current–voltage characteristics of our vacuum tube. At $x = L$ (where L is the inter-electrode spacing), let the potential be V volts. Then we can solve equation (1.15) for the current density:

$$j = -\frac{4\epsilon_0}{9L^2}\left(\frac{2e}{m_e}\right)^{1/2} V^{3/2}. \tag{1.16}$$

Finally, let us evaluate the performance of a specific configuration. Let us take a fairly large tube: an inter-electrode spacing of 0.01 m, and an electrode area of $0.05\,\text{m} \times 0.20\,\text{m} = 0.01\,\text{m}^2$. For a voltage drop of 50 V, we get a current drain of $8.3\,\text{A m}^{-2}$, or only 83 mA—we need much larger electric fields to draw significant power in a vacuum tube. The cloud of electrons at a density of about $2 \times 10^{13}\,\text{m}^{-3}$ impedes the flow of current rather effectively. For perspective, note that a tungsten cathode of this area can provide an emission current of hundreds of amperes.

1.5 THE ARC DISCHARGE

We have now in our vacuum tube a population of electrons with energies up to 50 eV. Let us imagine introducing gas at a pressure of $\sim$ 1 Pa (about 10^{-5} of an atmosphere). The electrons emitted from the cathode will collide with the gas molecules, transferring momentum and energy efficiently to the bound electrons within these gas molecules. Since typical binding energies of outer-shell electrons are in the few eV range, these collisions have a good probability of ionizing the gas, resulting in more free electrons. The 'secondary' electrons created in this way are then heated by collisions with the incoming primary electrons from the hot cathode, and cause further ionizations themselves. Eventually the ions and electrons come into thermal equilibrium with each other at temperatures corresponding to particle energies in the range of 2 eV, in the plasma generated in such an 'arc' discharge. Since most of the electrons are now thermalized—not monoenergetic as in the Child–Langmuir problem—they have a range of velocities. The energy of some of the secondary electrons, as well as that of the primaries, is high enough to continue to cause ionization. This continual ionization process balances the loss of ions which drift out of the plasma and recombine with electrons at the cathode or on the walls of the discharge chamber, and the system comes into steady state. Ion and electron densities in the range of $10^{18}\,\text{m}^{-3}$ are easily obtained in such a system.

Matters have changed dramatically from the original Child–Langmuir problem. The electron density has risen by five orders of magnitude, but

nonetheless the space-charge effect impeding the flow of the electron current is greatly reduced. The presence of the plasma, which is an excellent conductor of electricity, greatly reduces the potential gradient in most of the inter-electrode space. Only in the region close to the cathode are the neutralizing ions absent—because there they are rapidly drawn into the cathode by its negative potential. Almost all of the potential drop occurs then across this narrow 'sheath' in front of the cathode. If we return to equation (1.16), we see that the current extracted from the cathode must then increase by about the ratio $(L/\lambda_s)^2$, where λ_s is the width of the cathode sheath.

The current–voltage characteristic of an arc plasma is very different from the Child–Langmuir relation: indeed in a certain sense its resistance is negative. The external circuit driving the arc must include a resistive element as well as a voltage source. If the resistance of this element is reduced, allowing *more current* to flow through the arc, the plasma density increases due to the increased input power, the cathode sheath narrows due to the higher plasma density, *and the voltage drop across the arc falls!* Of course even though the voltage decreases with rising current, the input power, IV, increases. This nonetheless strange situation pertains up to the point where the full electron emission from the cathode is drawn into the arc. The voltage drop at this point might be 10–20 V in our case, the current hundreds of amperes, and the input power would be thousands of watts. If the current is raised further the arc makes the transition from space-charge-limited to emission-limited, and the voltage across the arc rises with rising current, since a higher voltage is needed to pull ions into the cathode.

Thus, as we can see, by introducing gas—and therefore plasma—into the problem, we have created a very different situation. From an engineering point of view, we now have to consider how to handle kilowatts of heat outflow from a small volume. From a physics point of view, it is interesting now to try to understand the behavior of the new state of matter we have just created.

Of course we do not always have to make a plasma in order to study one. The Sun is a plasma; so are the Van Allen radiation belts surrounding the Earth. The solar wind is a streaming plasma that fills the solar system. These plasmas in our solar system provide many unsolved mysteries. How is the Sun's magnetic field generated, and why does it flip every eleven years? How is the solar corona heated to temperatures greater than the surface temperature of the Sun? What causes the magnetic storms that result in a rain of energetic particles into the Earth's atmosphere, and disturbances in the Earth's magnetic field? Outside of the solar system there are also many plasma-related topics. What is the role of magnetic fields in galactic dynamics? The signals from pulsars are thought to be synchrotron radiation from rotating, highly magnetized neutron stars. What can we learn from these signals about the atmospheres of neutron stars and about the interstellar medium? All of these are very active areas of research.

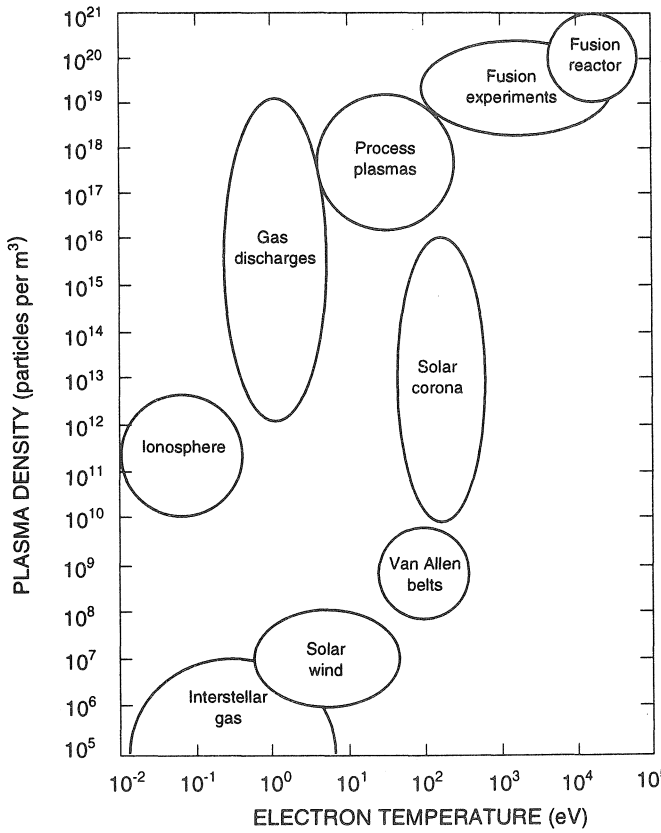

Figure 1.3. Typical parameters of naturally occurring and laboratory plasmas.

Some typical parameters of naturally occurring and laboratory plasmas are given in Table 1.1. Their density and temperature parameter regimes are illustrated in Figure 1.3. We see that the plasma state spans enormous ranges in scale-length, density of particles and temperature.

1.6 THERMAL DISTRIBUTION OF VELOCITIES IN A PLASMA

If we have a plasma in some form of near-equilibrium, i.e. where the particles collide with each other frequently compared to the characteristic time-scale over which energy and particles are replaced, it is reasonable to expect the laws of equilibrium statistical mechanics to give a good approximation to the distribution of velocities of the particles. We will assume for the time being that the distribution with respect to space is uniform.

Table 1.1. Typical parameters of naturally occurring and laboratory plasmas.

	Length scale (m)	Particle density (m^{-3})	Electron temperature (eV)	Magnetic field (T)
Interstellar gas	10^{16}	10^{6}	1	10^{-10}
Solar wind	10^{10}	10^{7}	10	10^{-8}
Van Allen belts	10^{6}	10^{9}	10^{2}	10^{-6}
Earth's ionosphere	10^{5}	10^{11}	10^{-1}	3×10^{-5}
Solar corona	10^{8}	10^{13}	10^{2}	10^{-9}
Gas discharges	10^{-2}	10^{18}	2	—
Process plasmas	10^{-1}	10^{18}	10^{2}	10^{-1}
Fusion experiment	1	10^{19}–10^{20}	10^{3}–10^{4}	5
Fusion reactor	2	10^{20}	10^{4}	5

Consider any one specific particle, labeled 'r', in the plasma as a distinguishable microsystem. We will ignore quantum-mechanical effects that make distinguishability invalid, and consider only particles that behave classically.

Problem 1.1: What are some plasma parameters (electron temperatures and densities) where quantum-mechanical effects might be important?

We now ask the question: what is the probability P_r of finding our specific particle in any *one* particular state of energy W_r? The particle has to have gained this energy W_r from its interaction with the others, so the remaining thermal 'bath' of particles must have energy $W_{\text{tot}} - W_r$, where W_{tot} is the total thermal energy in the plasma. If the particles have collided with each other enough, we can expect the fundamental theorem of statistical mechanics to hold. This theorem amounts to saying that we know as little as could possibly be known about any given thermal system: all possible accessible microstates of the total system are populated with equal probability. Thus in order to determine the probability P_r of any given state of our specific particle, we need only evaluate the number of microstates accessible to the 'bath' with energy $W_{\text{tot}} - W_r$. Let us define Ω as the number of microstates accessible to the bath with total energy W. Then, for any thermal system statistical mechanics *defines* its temperature,

T, by the relation

$$\frac{1}{T} \equiv \frac{k\,\mathrm{d}\ln\Omega}{\mathrm{d}W} \equiv \frac{\mathrm{d}S}{\mathrm{d}W} \tag{1.17}$$

where k is the Boltzmann constant, and the entropy, S, of the system is defined by $S \equiv k\ln\Omega$. Since the energy of our specific particle is small compared to the energy of the bath, we can approximate the number of microstates available to the system by

$$\ln\ \Omega|_{W_{\mathrm{tot}}-W_r} \approx \ln\ \Omega|_{W_{\mathrm{tot}}} - W_r/kT. \tag{1.18}$$

Taking the exponential of both sides, we obtain

$$\Omega|_{W_{\mathrm{tot}}-W_r} \approx \Omega\,|_{W_{\mathrm{tot}}} \exp(-W_r/kT) \tag{1.19}$$

which is just the result we are seeking. The relative probability P_r of the particle having energy W_r is given by the famous 'Boltzmann factor', $\exp(-W_r/kT)$, since Ω evaluated at W_{tot} is not a function of W_r.

If we ignore, for the time being, any potential energy associated with the position of the particle, we have the result that the relative probability that the velocity of our particle lies in some range of velocities $\mathrm{d}v_x\mathrm{d}v_y\mathrm{d}v_z$ centered around velocity (v_x, v_y, v_z) is given by

$$\exp\left(\frac{-m(v_x^2+v_y^2+v_z^2)}{2kT}\right)\mathrm{d}v_x\mathrm{d}v_y\mathrm{d}v_z \tag{1.20}$$

where m is the mass of the particle. Since there was nothing special about our particular particle (which was chosen arbitrarily from the bath), this same relative probability distribution is appropriate for all the particles in the bath. It is convenient to define a 'phase-space density of particles', $f(\mathbf{x}, \mathbf{v})$, which gives the number of particles per unit of $\mathrm{d}x\mathrm{d}y\mathrm{d}z\mathrm{d}v_x\mathrm{d}v_y\mathrm{d}v_z$, the volume element of six-dimensional phase space. The three-dimensional integral of f over all velocities, $\mathbf{v}$, gives the number density of particles per unit volume of ordinary physical space, which we denote n. The units of f are given by

$$[f] = \mathrm{m}^{-3}(\mathrm{m\,s}^{-1})^{-3} = \mathrm{s}^3\,\mathrm{m}^{-6}. \tag{1.21}$$

For a Maxwell–Boltzmann distribution, f is simply the Boltzmann factor with an appropriate normalization. If we carry through the necessary integral over all $\mathbf{v}$ to ensure that

$$\int f\mathrm{d}v_x\mathrm{d}v_y\mathrm{d}v_z = n \tag{1.22}$$

thereby obtaining the correct normalizing factor, the result is that the Maxwell–Boltzmann (or Maxwellian) distribution function is given by

$$f_{\mathrm{M}} = \frac{n}{(\sqrt{2\pi}\,v_{\mathrm{t}})^3}\exp(-v^2/2v_{\mathrm{t}}^2) \tag{1.23}$$

where the thermal velocity, v_t, is given by

$$v_t \equiv (kT/m)^{1/2}. \tag{1.24}$$

Equation (1.24) is the last time that we will show the Boltzmann constant, k. Henceforth we will drop k, writing for example simply $v_t = (T/m)^{1/2}$. The Boltzmann constant k has the role of converting temperature from degrees Kelvin to units of energy (see equation (1.17)). In plasma physics, we generally find it more convenient to express temperature directly in energy units. In practical applications, we tend to discuss the temperature in units of electron-volts (eV), the kinetic energy an electron gains in free-fall down a potential of 1 V, but the equations we write, such as $v_t = (T/m)^{1/2}$ above, are in SI units for velocity and mass, so T is expressed in joules. Since when a charge of one coulomb falls down a potential of one volt, the kinetic energy gain is by definition one joule, the energy in an electron-volt, expressed in joules, is numerically equal to the electron charge expressed in coulombs. Rather than refer to a plasma as having temperature 11 600 K, we say its temperature is 1 eV, and evaluate T in SI units as 1.60×10^{-19} J (see Appendix C). Often, however, we will encounter the expressions (T/e) or (W/e) in plasma physics equations. When evaluating such expressions, it is even more convenient to insert the temperature, T, or particle energy, W, in units of eV, for the whole expression. An eV divided by e is a V—a perfectly good unit in SI! In other words, the expression (W/e) for a 10 keV particle becomes in SI 10^4 V. Remember, however, that the average kinetic energy of a particle in a Maxwellian distribution is $\langle W \rangle = (3/2)kT$—or, in our nomenclature, $\langle W \rangle = (3/2)T$. This is because the distribution contains three degrees of freedom per particle, corresponding to the three velocity components (v_x, v_y, v_z). From statistical mechanics we know that the typical energy associated with each degree of freedom is $T/2$.

One important use of the velocity-space distribution function f is to find the value of some quantity averaged over the distribution. For any quantity X, the local velocity-space average of X, which we denote $\langle X \rangle_v$ is given by

$$\langle X \rangle_v = \frac{\int f X \mathrm{d}^3 v}{\int f \mathrm{d}^3 v} = \frac{\int f X \mathrm{d}^3 v}{n}. \tag{1.25}$$

In particular, if we take $X = W \equiv mv^2/2$, we find, for a Maxwellian distribution, that $\langle W \rangle_v = (3/2)T$, as we discussed above. If we are interested in the average energy of motion that a particle has in any one direction, say the z direction, $W_z \equiv mv_z^2/2$, we find $\langle W_z \rangle_v = T/2$ for a Maxwellian distribution function. The average of v_z^2 is simply T/m, or v_t^2 as defined by equation (1.24). Thus the quantity v_t, as we have defined it, is the 'root-mean-square' of the velocities in any one direction. (Beware that some researchers use an alternative definition, namely $v_t \equiv (2T/m)^{1/2}$.)

In some cases, a plasma has an anisotropic distribution function, which can be approximated as a 'bi-Maxwellian' with a different temperature along the magnetic field than across the field. This can happen in the laboratory or in natural plasmas due to forms of heating that add perpendicular or parallel energy preferentially to the particles, or loss processes that take out one or the other form of energy rapidly compared to collisions. In this case, taking the direction of the magnetic field to be the z direction, we have

$$f = \frac{n}{(\sqrt{2\pi}\, v_{t\parallel})(\sqrt{2\pi}\, v_{t\perp})^2} \exp\left(-\frac{v_z^2}{2v_{t\parallel}^2} - \frac{v_x^2 + v_y^2}{2v_{t\perp}^2}\right) \tag{1.26}$$

where

$$v_{t\perp} \equiv (T_\perp/m)^{1/2} \qquad v_{t\parallel} \equiv (T_\parallel/m)^{1/2} \tag{1.27}$$

and $\langle W_z\rangle_v = \langle W_\parallel\rangle_v = m\langle v_\parallel^2\rangle_v/2 = T_\parallel/2$, because the parallel direction represents one degree of freedom. Similarly, defining $v_\perp^2 = v_x^2 + v_y^2$, $\langle W_x\rangle_v = \langle W_y\rangle_v = m\langle v_\perp^2\rangle_v/4 = T_\perp/2$, so $\langle W_\perp\rangle_v = \langle W_x\rangle_v + \langle W_y\rangle_v = T_\perp$, because the perpendicular direction represents two degrees of freedom. In an isotropic plasma, with $T_\parallel = T_\perp = T$, $\langle W_\perp\rangle_v = 2\langle W_\parallel\rangle_v$.

Problem 1.2: Sketch a three-dimensional plot of an anisotropic distribution function f, with $T_\parallel = 2T_\perp$. Show that $\int f\mathrm{d}^3v = n$ for f given by equation (1.26).

1.7 DEBYE SHIELDING

We have now done some very basic statistical mechanics to understand the Maxwell–Boltzmann distribution function of a plasma. Maxwell–Boltzmann statistics arise repeatedly in plasma physics, and the next example is fundamental to the very definition of a plasma. Consider a charge artificially immersed in a plasma which is in thermodynamic equilibrium. The equilibrium state implies that the plasma must be changing very slowly compared to the particle collision time, and that there is no significant temperature variation over distances comparable to a collision mean-free path. For present purposes, we will assume that the plasma is 'isothermal'—at a constant temperature, independent of position. Once again, consider the particle distribution function to be a heat 'bath' at a given temperature. And again consider a single specific particle, but now allow the particle to have both kinetic and potential energy:

$$W_r = mv^2/2 + q\phi \tag{1.28}$$

where q is the charge of the particle ($-e$ for an electron, $+Ze$ for an ion of charge Z), and so the Boltzmann factor becomes

$$\exp[-(mv^2/2 + q\phi)/T]. \tag{1.29}$$

The relative probability of a given energy of the particle now depends on position implicitly, through ϕ. The point worth noting is that this same Boltzmann factor (with a constant normalization in front—independent of position) gives the relative probability and therefore the relative particle distribution function over the whole volume in thermal equilibrium. If we integrate the distribution function over velocity space to obtain a relative local particle density, we find that the spatial dependence that remains comes only from the Boltzmann factor:

$$n \propto \exp(-q\phi/T). \tag{1.30}$$

This means physically that electrons will tend to gather near a positive charge in a plasma, and therefore they will tend to shield out the electric field from the charge, preventing the field from penetrating into the plasma. By the same token, ions will have the opposite tendency, to 'shy away from' a positive charge, and gather near a negative one.

A fundamental property of a plasma is the distance over which the field from such a charge is shielded out. Indeed, it is considered one of two formal defining characteristics of a plasma that this shielding length (called the Debye length, λ_D, which was first calculated in the theory of electrolytes by Debye and Hückel in 1923) be much smaller than the plasma size. The second defining characteristic of a plasma is that there should be many particles within a Debye sphere, which has volume $(4/3)\pi\lambda_D^3$, with the consequence that the statistical treatment of Debye shielding is valid.

It is fairly easy to calculate the Debye length for an idealized system. Let us suppose that we have immersed a planar charge in a plasma. Assume the plasma ions have charge Ze, and far from the electrode the ion and electron densities are $n_e = Zn_i \equiv n_{e\infty}$. This boundary condition at infinity is required in order to provide charge neutrality over the bulk of the plasma, so as to keep the electric field, $\mathbf{E}$, from building up indefinitely. Let us also choose to set $\phi = 0$ at infinity for simplicity. Given our assumptions at infinity, from the Boltzmann factor we know that

$$\begin{aligned} n_e(x) &= n_{e\infty}\exp(e\phi/T_e) \\ Zn_i(x) &= n_{e\infty}\exp(-eZ_i\phi/T_i). \end{aligned} \tag{1.31}$$

We are allowing $T_e \neq T_i$, for generality, but both T_i and T_e are spatially homogeneous, i.e. the electrons are in thermal equilibrium among themselves,

and the ions are in thermal equilibrium among themselves, but the ions and electrons are not necessarily in thermal equilibrium with each other. At first sight this may seem unphysical, but it happens often in plasmas because electron–electron energy transfer by collisions and ion–ion energy transfer by collisions are both faster than collisional electron–ion energy transfer, due to the large mass discrepancy. We will study this in Unit 3. For the time being, it might be helpful to think about the example of collisional equilibration in a system of ping-pong balls and bumper-cars. At first the ping-pong balls and bumper-cars will each, separately, come to thermal equilibrium, because their self-collisions are efficient at transferring energy as well as momentum. It will take longer for the balls and cars to come into thermal equilibrium with each other, because the transfer of energy in their collisions is weak.

The Poisson equation for our one-dimensional planar geometry is

$$\epsilon_0 \frac{\mathrm{d}^2\phi}{\mathrm{d}x^2} = e(n_\mathrm{e} - Zn_\mathrm{i}) = en_{\mathrm{e}\infty}[\exp(e\phi/T_\mathrm{e}) - \exp(-eZ\phi/T_\mathrm{i})] \tag{1.32}$$

where ϵ_0 is again the permittivity of free space. It is difficult to solve this equation in the region near the planar charge, where $e\phi/T$ may be large, but we can obtain a qualitative sense of the solution by assuming that $e\phi/T$ is small, and expanding the exponential in $e\phi/T$. Equation (1.32) then becomes

$$\epsilon_0 \frac{\mathrm{d}^2\phi}{\mathrm{d}x^2} \approx en_{\mathrm{e}\infty}(e\phi/T_\mathrm{e} + eZ\phi/T_\mathrm{i}) \tag{1.33}$$

i.e.

$$\frac{\mathrm{d}^2\phi}{\mathrm{d}x^2} \approx \frac{e^2 n_{\mathrm{e}\infty}(1 + ZT_\mathrm{e}/T_\mathrm{i})}{\epsilon_0 T_\mathrm{e}}\phi \tag{1.34}$$

which can be solved to obtain the characteristic exponential decay length which we are seeking:

$$\phi \propto \exp(-x/\lambda_\mathrm{D}) \tag{1.35}$$

where

$$\lambda_\mathrm{D} \equiv \left(\frac{\epsilon_0 T_\mathrm{e}}{n_\mathrm{e} e^2(1 + ZT_\mathrm{e}/T_\mathrm{i})}\right)^{1/2} \tag{1.36}$$

Often the ion term is not included in the definition of the Debye length, giving $\lambda_\mathrm{D} \equiv (\epsilon_0 T_\mathrm{e}/n_\mathrm{e} e^2)^{1/2}$. For typical laboratory plasmas, the Debye length is indeed small. For a 3 eV electric arc discharge at a density of $10^{19}\,\mathrm{m}^{-3}$, we find that $\lambda_\mathrm{D} \approx 3 \times 10^{-6}$ m. The number of particles in the Debye sphere for this case is about one thousand, making our statistical treatment reasonably valid.

Problem 1.3: Derive the equivalent of equation (1.34) in spherical coordinates (i.e. for the case of a point charge immersed in a plasma). Show that the solution is $\phi \propto \exp(-r/\lambda_\mathrm{D})/r$.

Problem 1.4: The typical distance between two electrons in a plasma is of order $n_e^{-1/3}$. Show that the potential energy associated with bringing two electrons this close together is much less than their typical kinetic energy, so long as $n_e\lambda_D^3 \gg 1$.

1.8 MATERIAL PROBES IN A PLASMA

In our discussion of Debye shielding, we considered the response of an equilibrium plasma to a localized charge. We did not, however, consider the possibility of collisions between plasma particles and whatever was carrying the charge. The situation is very different in the case of a real material probe inserted into a plasma. Such a probe intercepts particle trajectories, resulting in violation of the assumption of equilibrium in its near vicinity. If the probe is biased negative with respect to the plasma, with potential $\phi \ll -T_e/e$, few electron trajectories are intercepted, since most electrons cannot reach the probe, so the electrons will be close to equilibrium and maintain $n_e \sim n_{e\infty}\exp(e\phi/T)$. A sheath region will develop around the probe, whose width scales with the Debye length, as in the case we just considered, because the electron population will be exponentially depleted close to the negatively biased probe. Ions, however, will be accelerated across the sheath, and into the material electrode. In the case of cold ions, $T_i \ll T_e$, the calculation of the ion density reduces to the ion analog of the Child–Langmuir calculation we performed at the beginning of this Chapter. While the electron density falls exponentially in the vicinity of a negatively biased material probe, the ion density is depressed as well, but more weakly, as $\phi^{-1/2}$ (see equation (1.12)). The ion density, in this case, is *not* enhanced by the negative bias, due to the depleting collisions with the probe surface. The ion current density to a negatively biased probe in a $Z = 1$ plasma is given approximately by $j_i \sim n_{i\infty}eC_s$, where C_s is the so-called 'ion sound speed' $C_s \equiv [(T_e + T_i)/m_i]^{1/2}$, which shows up in situations like this where both ion and electron temperatures contribute to ion motion, and $n_{i\infty}$ is the ion density far from the probe. (We will encounter C_s again when we study ion acoustic waves in Unit 4.) This ion current is called the 'ion saturation current', $j_{sat,i}$, because the ion current saturates at this value as the probe bias is driven further negative. The sheath width grows as the potential becomes more negative, in just such a way as to keep the ion Child–Langmuir current constant at $j_{sat,i}$.

Problem 1.5: Perform an ion Child–Langmuir calculation to model the plasma sheath at a material probe. Assume an inter-electrode spacing of $\lambda_D \equiv (\epsilon_0 T_e/n_e e^2)^{1/2}$ to model the sheath width, and a potential drop of $e\phi = -T_e$. Take $T_i = 0$. You may assume that the electron density is

negligible in the sheath region, to make the *ion* Child–Langmuir calculation valid. Determine the ion current density, j_i, across this model sheath.

The electron current to a material probe depends exponentially on the probe potential, since the electron density at the probe face varies exponentially with $e\phi/T$, and the particle flux from a Maxwell–Boltzmann electron distribution into a material wall is given by Γ [particles s^{-1} m^{-2}] $= n_e(8T_e/\pi m_e)^{1/2} \sim n_e v_{t,e}$. A potential of $e\phi \sim 3.3T_e$ is required to reduce the electron current to the probe to equal the ion current, in a hydrogen plasma. This is called the 'floating' potential, because the potential of a probe that is not allowed to draw any net current will 'float' to this value. Such a strong potential is required, of course, because $v_{t,e} \sim C_s(m_i/m_e)^{1/2}$, so the electron current in the absence of negative probe bias is much larger in absolute magnitude than $j_{sat,i}$.

UNIT 1

SINGLE-PARTICLE MOTION

In this Unit we will investigate charged-particle motion in magnetic, electric and even gravitational fields. Natural and laboratory-generated plasmas are frequently immersed in strong externally-generated magnetic fields, because these fields confine charged-particle orbits (and therefore plasmas), at least in the direction perpendicular to the magnetic field. Magnetic and electric fields are also generated by currents and charge accumulations within plasmas, and so an understanding of charged-particle motion in these fields underlies the understanding of the dynamics of plasma motion.

We will begin by studying particle motion in uniform static fields in Chapter 2. Then we will include spatial gradients in Chapter 3. In Chapter 4 we will include time-dependent phenomena, and discuss invariants of particle motion. In Chapter 5 we will introduce the modern nonlinear theory of chaos in particle orbits, using the concept of Hamiltonian maps.

Chapter 2

Particle drifts in uniform fields

Many plasmas are immersed in externally imposed magnetic and/or electric fields. All plasmas have the potential to generate their own electromagnetic fields as well. Thus, as a first step towards understanding plasma dynamics, in this Chapter we begin by considering the behavior of charged particles in uniform fields, thus constructing the most fundamental aspects of a magnetized plasma. We also carefully introduce some of the mathematical formalisms that we will use throughout the book.

2.1 GYRO-MOTION

In the presence of a uniform magnetic field, the equation of motion of a charged particle is given by

$$m\dot{\mathbf{v}} = q\mathbf{v} \times \mathbf{B} \tag{2.1}$$

where q is the (signed) charge of the particle. Taking $\hat{\mathbf{z}}$ to be the direction of $\mathbf{B}$ (i.e. $\mathbf{B} = B\hat{\mathbf{z}}$ or we sometimes say $\hat{\mathbf{b}} \equiv \mathbf{B}/B$ which, in this case, is the same as $\hat{\mathbf{z}}$), we have

$$\dot{v}_x = qv_yB/m \tag{2.2}$$

$$\dot{v}_y = -qv_xB/m \tag{2.3}$$

$$\dot{v}_z = 0. \tag{2.4}$$

For a specific trajectory, we also need initial conditions at $t = 0$: these we take to be $x = x_i$, $y = y_i$, $z = z_i$, $v_x = v_{xi}$, $v_y = v_{yi}$, $v_z = v_{zi}$. If we take the time derivative of both sides of equation (2.2), we can use equation (2.3) to substitute for $\dot{v}_y$, and obtain

$$\frac{\mathrm{d}^2v_x}{\mathrm{d}t^2} = -\left(\frac{qB}{m}\right)^2 v_x. \tag{2.5}$$

If we define $\omega_c \equiv |q|B/m$, it is clear that the solution of this equation is

$$v_x = A\cos(\omega_c t) + B\sin(\omega_c t) \tag{2.6}$$

where A and B are integration constants. Evidently ω_c, called the 'cyclotron frequency' (also sometimes called the 'Larmor frequency' or the 'gyro-frequency'), is going to prove to be a very important quantity in a magnetized plasma. It is convenient to use complex-variable notation, and rewrite equation (2.6) as

$$\begin{aligned} v_x &= \mathrm{Re}[A\exp(\mathrm{i}\omega_c t)] - \mathrm{Re}[B\mathrm{i}\exp(\mathrm{i}\omega_c t)] \\ &= \mathrm{Re}\left[(A - \mathrm{i}B)\exp(\mathrm{i}\omega_c t)\right] = \mathrm{Re}\left\{\left[v_\perp \exp(\mathrm{i}\delta)\right]\exp(\mathrm{i}\omega_c t)\right\} \\ &= \mathrm{Re}\left[v_\perp \exp(\mathrm{i}\omega_c t + \mathrm{i}\delta)\right] \end{aligned} \tag{2.7}$$

where Re indicates the real part of the subsequent expression, $v_\perp$ is an absolute speed perpendicular to $\mathbf{B}$, and δ is a phase angle. The quantities $v_\perp$ and δ have become our new integration constants. (We will now drop the Re in this notation, since it is clear that we are dealing with real quantities.) In this formulation, $v_\perp$ and δ are chosen to match the initial velocity conditions. Equation (2.2) gives

$$v_y = \mathrm{i}(|q|/q)v_\perp \exp(\mathrm{i}\omega_c t + \mathrm{i}\delta) = \pm \mathrm{i} v_\perp \exp(\mathrm{i}\omega_c t + \mathrm{i}\delta) \tag{2.8}$$

where $\pm$ evidently indicates the sign of q. From the initial conditions, we now can say that $v_\perp = (v_{xi}^2 + v_{yi}^2)^{1/2}$ and $\delta = \mp\tan^{-1}(v_{yi}/v_{xi})$, where the upper sign is for positive q. Note that v_x and v_y are 90° out of phase, so we have circular motion in the plane perpendicular to $\mathbf{B}$. Equation (2.4) indicates that v_z is a constant, and so the motion constitutes a helix along $\mathbf{B}$. If we integrate equations (2.4), (2.7) and (2.8) in time, we obtain

$$\begin{aligned} x &= x_i - \mathrm{i}(v_\perp/\omega_c)[\exp(\mathrm{i}\omega_c t + \mathrm{i}\delta) - \exp(\mathrm{i}\delta)] \\ y &= y_i \pm (v_\perp/\omega_c)[\exp(\mathrm{i}\omega_c t + \mathrm{i}\delta) - \exp(\mathrm{i}\delta)] \\ z &= z_i + v_{zi} t \end{aligned} \tag{2.9}$$

where the integration constants have been chosen to match the initial position conditions.

Clearly, then, another fundamental quantity in a magnetized plasma is the length $r_L \equiv (v_\perp/\omega_c)$, called the 'Larmor radius' or 'gyro-radius'. This is the radius of the helix described by the particle as it travels along the magnetic field line. Figure 2.1 shows an electron and a proton gyro-orbit, drawn more or less to scale, for equal particle energies $W = mv_\perp^2/2$. The ratio of the two gyro-radii is the square-root of the ratio of the proton mass to the electron mass, $\sqrt{1837} \approx 43$. Note that $v_\perp$ is proportional to $(W/m)^{1/2}$, and ω_c is proportional to $1/m$, so r_L is proportional to $(mW)^{1/2}$.

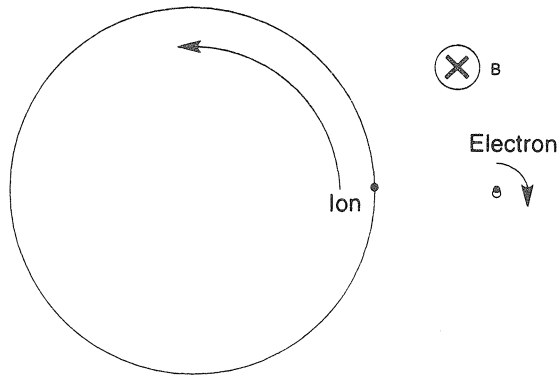

Figure 2.1. Ion and electron gyro-motion in a magnetic field. For fixed energy, the ion's gyro-orbit is much larger than the electron's. 'X' indicates that the magnetic field faces into the page.

The centers of the gyro-orbits are referred to as their 'guiding centers', or 'gyro-centers', and give a measure of a particle's average location during a gyro-orbit. Averaging equation (2.9) over a gyro-period, the guiding-center position for the particular initial values considered here is seen to be given by

$$x_{gc} = x_i + i(v_\perp/\omega_c)\exp(i\delta) \qquad y_{gc} = y_i \mp (v_\perp/\omega_c)\exp(i\delta) \tag{2.10}$$

so that the particle's position described in terms of its guiding-center position is given by

$$\begin{aligned} x &= x_{gc} - i(v_\perp/\omega_c)\exp(i\omega_c t + i\delta) \\ y &= y_{gc} \pm (v_\perp/\omega_c)\exp(i\omega_c t + i\delta) \\ z &= z_{gc} = z_i + v_{zi}t. \end{aligned} \tag{2.11}$$

Thus we can think of particle gyro-centers as sliding along magnetic field lines, like beads on a wire. Note that electrons and ions rotate around the field lines in opposite directions, with the upper sign giving the phase for positively charged particles. If you point your two thumbs along the direction of the magnetic field, the fingers of your left hand curl in the direction of rotation of positively charged ions, while those of your right hand do the same for electrons. These directions of rotation are both such that the tiny perturbation of the magnetic field inside the particle orbits, due to the current represented by the particle motion, acts to *reduce* the ambient magnetic field. High-pressure plasmas reduce the externally imposed magnetic field through the superposition of this 'diamagnetic' effect from a high density of energetic particles.

The ion and electron Larmor radii and gyro-frequencies provide fundamental space-scales and time-scales in a magnetized plasma. Phenomena

which occur on space-scales much smaller than the gyro-radius, or on time-scales much faster than a gyro-period, are often insensitive to the presence of the magnetic field, and can be described using equations appropriate for an unmagnetized plasma. In the opposite limit of large space-scales and long time-scales, gyro-motion is crucial to plasma behavior, and generates some surprising phenomena—somewhat akin to the behavior of a gyroscope which responds to any attempt to change the orientation of its axis of rotation by moving at 90° to the applied torque. Some plasma phenomena, especially in the Earth's magnetosphere, can occur at *intermediate* space-scales and time-scales, such that the electrons can be considered magnetized, while the ions are essentially unmagnetized. In our discussion of particle motion, however, we will generally consider space-scales much greater than a gyro-radius, and time-scales much longer than a gyro-period of either species, unless we specifically state otherwise.

Problem 2.1: Look through articles in *Physical Review Letters, Plasma Physics, Physics of Fluids* B (recently renamed *Physics of Plasmas*) or in other journals over recent years and find at least one article each about laboratory, solar or terrestrial, and astrophysical plasmas immersed in magnetic fields. Give the reference and a few-sentence description of each article. For the plasmas you find described, evaluate the ion and electron gyro-radii and the Debye radius (ignoring ion shielding), insofar as the authors give you the required information. Compare these to the system sizes. Calculate how many particles are within a Debye sphere for each case. Evaluate the ion and electron cyclotron frequencies and compare to the evolution time-scale of the overall plasma. Which of these systems are really plasmas? Which of these are magnetized versus unmagnetized plasmas?

2.2 UNIFORM E FIELD AND UNIFORM B FIELD: E × B DRIFT

Starting from the configuration we have just discussed, with $\mathbf{B} = B\hat{\mathbf{z}}$, let us add a uniform electric field $\mathbf{E}$. We will assume that both the electric and the magnetic field are time-independent. The non-relativistic equation of motion becomes

$$m\dot{\mathbf{v}} = q(\mathbf{E} + \mathbf{v} \times \mathbf{B}). \tag{2.12}$$

Now we will employ a mathematical transformation, which we will justify later, in order to solve this equation expeditiously. Let us define a velocity $\mathbf{u}$ by

$$\mathbf{u} \equiv \mathbf{v} - (\mathbf{E} \times \mathbf{B})/B^2. \tag{2.13}$$

In other words, $\mathbf{u}$ is the particle velocity that we would see in a frame moving at velocity $(\mathbf{E} \times \mathbf{B})/B^2$. Since $\mathbf{E}$ and $\mathbf{B}$ are time-independent, we have $\dot{\mathbf{v}} = \dot{\mathbf{u}}$

and so, substituting for $\mathbf{v}$ in terms of $\mathbf{u}$, equation (2.12) for $\dot{\mathbf{u}}$ becomes

$$m\dot{\mathbf{u}} = q[\mathbf{E} + \mathbf{u} \times \mathbf{B} + (\mathbf{E} \times \mathbf{B}) \times \mathbf{B}/B^2]. \tag{2.14}$$

Now, we use the vector identity

$$(\mathbf{A} \times \mathbf{B}) \times \mathbf{C} = (\mathbf{A} \cdot \mathbf{C})\mathbf{B} - (\mathbf{B} \cdot \mathbf{C})\mathbf{A} \tag{2.15}$$

(see Appendix D) to obtain

$$\begin{aligned} m\dot{\mathbf{u}} &= q[\mathbf{E} + \mathbf{u} \times \mathbf{B} + (\mathbf{E} \cdot \mathbf{B})\mathbf{B}/B^2 - \mathbf{E}] \\ &= q[\hat{\mathbf{b}}(\mathbf{E} \cdot \hat{\mathbf{b}}) + \mathbf{u} \times \mathbf{B}]. \end{aligned} \tag{2.16}$$

To obtain the equation for the velocity *parallel* to $\mathbf{B}$, we take the dot-product of equation (2.16) with $\hat{\mathbf{b}}$, giving

$$m\dot{u}_\parallel = qE_\parallel \tag{2.17}$$

where we are defining

$$u_\parallel \equiv \mathbf{u} \cdot \hat{\mathbf{b}} \qquad E_\parallel \equiv \mathbf{E} \cdot \hat{\mathbf{b}} \qquad v_\parallel \equiv \mathbf{v} \cdot \hat{\mathbf{b}}. \tag{2.18}$$

From equation (2.13) we see that $u_\parallel = v_\parallel$, and so the solution for $v_\parallel$ is just free-fall in the electric field:

$$v_\parallel = (qE_\parallel/m)t + v_{\parallel i}. \tag{2.19}$$

To obtain the equation for the velocity *perpendicular* to $\mathbf{B}$, we multiply both sides of equation (2.17) by $\hat{\mathbf{b}}$, and subtract from equation (2.16). We obtain

$$m\dot{\mathbf{u}}_\perp = q\mathbf{u}_\perp \times \mathbf{B} \tag{2.20}$$

where $\mathbf{u}_\perp \equiv \mathbf{u} - u_\parallel\hat{\mathbf{b}}$, $\mathbf{E}_\perp \equiv \mathbf{E} - E_\parallel\hat{\mathbf{b}}$ and $\mathbf{v}_\perp \equiv \mathbf{v} - v_\parallel\hat{\mathbf{b}}$.

Thus, in the direction perpendicular to $\hat{\mathbf{b}}$, we have precisely the same equation for $\mathbf{u}$ as we had for $\mathbf{v}$ in the absence of an electric field, i.e. equation (2.11). We have found that the solution of this equation implies that the guiding center does not move at all perpendicular to $\mathbf{B}$, and we know that it slides along $\mathbf{B}$ with velocity $u_\parallel = v_\parallel$ as given by equation (2.19). Thus, in the frame moving at speed $(\mathbf{E} \times \mathbf{B})/B^2$, the only guiding-center velocity we see is parallel to $\mathbf{B}$, so in the laboratory frame we see a guiding-center velocity

$$\mathbf{v}_{\mathrm{gc}} = v_\parallel\hat{\mathbf{b}} + (\mathbf{E} \times \mathbf{B})/B^2 \equiv v_\parallel\hat{\mathbf{b}} + \mathbf{v}_E. \tag{2.21}$$

The velocity $\mathbf{v}_E \equiv \mathbf{E} \times \mathbf{B}/B^2$ is called the '$\mathbf{E} \times \mathbf{B}$ drift'. It is particularly easy to evaluate this drift in SI units: $\mathbf{E}$ is in units of volts/meter, $\mathbf{B}$ is evaluated in

units of teslas and $\mathbf{v}_E$ results in meters/second. Notice that $\mathbf{v}_E$ is independent of $q, m, v_\parallel$, and $v_\perp$. This means that the whole plasma drifts together across the electric and magnetic fields with the same velocity.

What we have actually done here is performed a simplified Lorentz transformation, using the $\mathbf{B}$ field to eliminate the $\mathbf{E}$ field in the moving frame, and so simplified the equation of motion. Of course the Lorentz transformation works the same for all particles, so the whole plasma $\mathbf{v}_E$-drifts together, relative to what it would have done without the $\mathbf{E}$ field. Since we have chosen to use a non-relativistic equation of motion, our Lorentz transformation is particularly simple. The approximation we have used is equivalent to assuming that $\gamma \equiv [1 - (v/c)^2]^{-1/2} \approx 1$, or $(v/c)^2 \ll 1$.

For a more physical picture of the origin of the $\mathbf{E} \times \mathbf{B}$ drift without resorting to the Lorentz transformation, consider how the particles are accelerated by the electric field during part of their gyro-orbits, and are decelerated during the other part. The result of these accelerations and decelerations is that the radii of curvature of the gyro-orbits will be slightly larger on the side where the particles have greater kinetic energy than on the side where the particles have less kinetic energy, due to having climbed a potential hill. This gives rise to a drift perpendicular to $\mathbf{E}$, as illustrated in Figure 2.2.

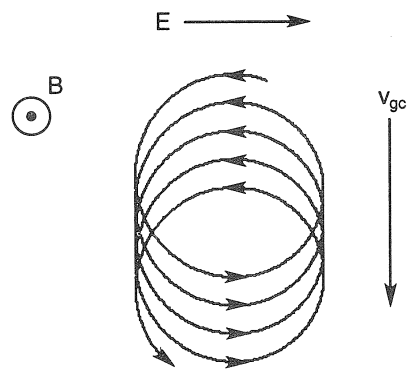

Figure 2.2. Electron $\mathbf{E} \times \mathbf{B}$ drift motion. The half-orbit on the left-hand side is larger than that on the right, because the electron has gained energy from the electric field. The dot indicates that the magnetic field faces out of the page.

Incidentally, in our derivation of the $\mathbf{E} \times \mathbf{B}$ drift, we did not have to assume anything about the relative size of v and $|\mathbf{v}_E|$. Indeed, the whole guiding center formalism can be developed for the case where $|\mathbf{v}_E|$ is of order v (at the expense of a greater complexity of terms), but we will hereafter assume $|\mathbf{v}_E| \ll v$ in our derivations.

2.3 GRAVITATIONAL DRIFT

In the presence of any other simple force on the charged particles in a plasma, we can apply directly the results we have derived for the electric force. In particular, if we imagine a plasma in the Earth's magnetic field, we might wonder what effect the Earth's gravity would have on it. We can simply replace the electric force $q\mathbf{E}$ with a general force, $\mathbf{F}$, in both the equation of motion and in its solution (e.g. in the definition of $\mathbf{u}$). This gives a guiding-center drift

$$\mathbf{v}_F = (\mathbf{F} \times \mathbf{B})/qB^2 \tag{2.22}$$

or, in the case of gravity, where $\mathbf{F} = m\mathbf{g}$,

$$\mathbf{v}_g = m(\mathbf{g} \times \mathbf{B})/qB^2 \tag{2.23}$$

which is usually called the 'gravitational drift'.

Note that $\mathbf{v}_g$, unlike $\mathbf{v}_E$, depends on m and q. The presence of gravity gives rise to a net current in a plasma; the ions drift one way and the electrons the other—the ions, which are much heavier, drift much faster. In a finite plasma, this current therefore gives rise to charge separation. Generally speaking, the actual gravitational drift $\mathbf{v}_g$ is very small, and we introduce it mainly for later application of the idea of a 'general force' drift to the case of centrifugal force.

It is interesting to ask why it is that a plasma 'cloud' above the Earth does not seem to fall down in the gravitational field. In fact, the gravitational drift is horizontal, not vertical! (Galileo, for one, might have found this disturbing.) The qualitative answer is that the ion and electron drifts are in opposite directions, and so if the plasma is finite in the horizontal direction, perpendicular to $\mathbf{B}$ and $\mathbf{g}$, charge separation occurs, an electric field builds up (in the horizontal direction and perpendicular to $\mathbf{B}$), and the plasma does indeed drift downwards, after all, due to the $\mathbf{v}_E$ drift. To analyze this situation quantitatively—and to determine whether the plasma falls with acceleration g—we must first understand how a plasma responds to a time-varying electric field, $\dot{\mathbf{E}}$. We will return to this topic in Chapter 4.

Problem 2.2: The ionosphere is composed mostly of a proton–electron plasma immersed in the Earth's magnetic field of about 3×10^{-5} T. How fast is the gravitational drift for each species?

Chapter 3

Particle drifts in non-uniform magnetic fields

In the previous Chapter, we studied particle drifts in uniform fields and developed the fundamental concepts of Larmor radius, gyro-frequency, and gyro-center motion. Now we consider magnetic field gradients both perpendicular and parallel to **B**, and curved magnetic fields. We will find gyro-center drifts across the magnetic field, and acceleration (or deceleration) along **B**. We will develop the concept of 'ordering' the drifts in the ratio of Larmor radius to gradient scale-length. To zeroth order, particles slide along **B** as before (but $v_\parallel$ will now vary), and to first order they drift across **B**, but they still precisely conserve the sum of potential and kinetic energy at each order.

3.1 ∇B DRIFT

We now proceed to examine particle guiding-center drifts in inhomogeneous magnetic fields. We will assume in all of these studies that the gyro-radius, r_L, is much less than the typical scale-length of variation of the magnetic field. Thus

$$\frac{r_L}{B}|\nabla B| \ll 1. \tag{3.1}$$

For example, if B has a sinusoidal variation, $B \propto \exp(ikx)$, or an exponential variation, $B \propto \exp(kx)$, this is equivalent to saying $kr_L \ll 1$, where $1/k$ is a characteristic gradient scale-length for the problem. In this situation, the quantity kr_L becomes a useful 'expansion parameter' for studying the equations of motion by the method of asymptotic expansion.

In our asymptotic expansion procedure, we will assume that the particle velocities can be expressed as a sum of terms

$$\mathbf{v} = \mathbf{v}_0 + \mathbf{v}_1 + \mathbf{v}_2 + \ldots \tag{3.2}$$

where the leading term is the particle's parallel velocity, $v_\parallel \hat{\mathbf{b}}$, plus its gyro-motion perpendicular to $\mathbf{B}$, and each successive term in the series is assumed to be smaller than the previous one, by approximately kr_L. We will be interested here in calculating the evolution of $\mathbf{v}_0$ and of $\mathbf{v}_1$, and in fact at first order we will only need the guiding-center motion averaged over many gyro-periods. Substituting our form for $\mathbf{v}$ into the equation of motion, we will find that we have terms in the equation *of each order*: $(kr_L)^0$, $(kr_L)^1$, $(kr_L)^2$, etc. If we solve for $\mathbf{v}_0, \mathbf{v}_1, \mathbf{v}_2$, etc., so as to make the terms in the equation of each order balance separately, we will have an asymptotic series solution for $\mathbf{v}$. This approach is justified by noting that, in the limit $kr_L \to 0$, terms of higher order in kr_L can never be used to balance terms of lower order, because for small enough kr_L, the higher-order terms must be negligible in comparison with the lower-order ones.

We begin by considering the case where we have a perpendicular (i.e. perpendicular to $\mathbf{B}$) gradient in the field strength, B. For simplicity let us assume that $\mathbf{B}$ is in the z direction, and varies only with y. (To generate this field, we need distributed volume currents, since $\nabla \times \mathbf{B} \neq 0$. Such currents are common in plasmas, but do not affect directly our analysis of particle drifts. Of more importance is the fact that our model field does not violate $\nabla \cdot \mathbf{B} = 0$.) We write

$$\mathbf{B} = B_{\mathrm{gc},i}\hat{\mathbf{z}} + (y - y_{\mathrm{gc},i})\frac{\mathrm{d}B}{\mathrm{d}y}\hat{\mathbf{z}} \tag{3.3}$$

where $y_{\mathrm{gc,i}}$ is the initial y position of the particle guiding-center, and $B_{\mathrm{gc},i}$ is the value of B at $y_{\mathrm{gc},i}$. We assume for the validity of our asymptotic expansion procedure that $r_L(\mathrm{d}B/\mathrm{d}y) \ll B$. The equations of motion in the perpendicular (x and y) directions are

$$\begin{aligned} m\dot{v}_x &= q v_y[B_{\mathrm{gc},i} + (y - y_{\mathrm{gc},i})(\mathrm{d}B/\mathrm{d}y)] \\ m\dot{v}_y &= -q v_x[B_{\mathrm{gc},i} + (y - y_{\mathrm{gc},i})(\mathrm{d}B/\mathrm{d}y)]. \end{aligned} \tag{3.4}$$

Substituting the series expansion for $\mathbf{v}$, we obtain

$$\begin{aligned} m\dot{v}_{x0} + m\dot{v}_{x1} &= q(v_{y0} + v_{y1})[B_{\mathrm{gc},i} + (y_0 - y_{\mathrm{gc},i})(\mathrm{d}B/\mathrm{d}y)] \\ m\dot{v}_{y0} + m\dot{v}_{y1} &= -q(v_{x0} + v_{x1})[B_{\mathrm{gc},i} + (y_0 - y_{\mathrm{gc},i})(\mathrm{d}B/\mathrm{d}y)]. \end{aligned} \tag{3.5}$$

We have ignored some of the terms that are second order in kr_L, but we have kept all terms that might prove to be of lower order.

In thinking carefully about this procedure, we encounter one of the interesting subtleties of using asymptotic expansions. We will *assume* that $(y - y_{\mathrm{gc},i})(\mathrm{d}B/\mathrm{d}y)$ is smaller than $B_{\mathrm{gc},i}$ by one order in kr_L. This requires that $(y - y_{\mathrm{gc},i})$ always be of order r_L for our series expansion to be correct. However that means that $y(t)$, which we do not yet know, must not grow without bound,

because in that case the quantity $(y - y_{gc,i})$ would not remain of order r_L, as our ordering assumes. In particular $y_1(t)$ must not grow without bound, so we must watch out for such 'secularities' in y. In the case at hand this turns out not to be a problem, as we will see; our solution will maintain $(y - y_{gc,i})$ of order r_L—so, *a posteriori*, our assumption will be proven correct. In more complex situations, special techniques may be needed to eliminate secularities, but a valid solution can often still be obtained via this asymptotic expansion procedure.

So let us proceed with our order-by-order solution of equation (3.5). The zeroth-order terms in equation (3.5) constitute simply the equations of motion in a homogeneous magnetic field, which we gave first in equations (2.2) and (2.3), and whose solution is given in equations (2.7), (2.8) and (2.11). Our procedure calls for us to assume that the zeroth-order terms balance, implying that the zeroth-order velocities and positions must be given by our previous solution. Next we gather together all the first-order terms (terms of order kr_L compared to the largest ones) to generate a first-order equation that we must solve:

$$\begin{aligned} m\dot{v}_{x1} &= qv_{y1}B_{gc,i} + qv_{y0}(y_0 - y_{gc,i})(dB/dy) \\ m\dot{v}_{y1} &= -qv_{x1}B_{gc,i} - qv_{x0}(y_0 - y_{gc,i})(dB/dy). \end{aligned} \tag{3.6}$$

To make further progress, we will now time-average both of these first-order equations over many gyro-periods, since we are only interested in the gyro-averaged particle motion, sometimes called the 'guiding-center drift'. We use the notation $\langle\ \rangle$ here to indicate a time average. The left-hand side of both equations can be set to zero, because all that survives the gyro-averaging process are the time derivatives of $m\langle v_{x1}\rangle$ and $m\langle v_{y1}\rangle$ *due to changes that are slow compared to a gyro-period*, with the result that these terms are now very small compared to the first terms on the right-hand side. We say that the gyro-averaging process 'annihilates' these terms on the left-hand side. In effect it *raises* them by one order, since only time derivatives slow compared to a gyro-period survive the averaging. However for present purposes, the resulting second-order time derivatives can be neglected. Next we note that $\langle v_{y0}(y_0 - y_{gc,i})\rangle = 0$, since equations (2.8) and (2.11) show that v_{y0} and $y_0 - y_{gc,i}$ are 90° out-of-phase, and of course, $\langle v_{y0}y_{gc,i}\rangle = 0$.

Problem 3.1: Prove that $\langle v_{y0}(y_0 - y_{gc,i})\rangle = 0$ for all δ.

Thus $\langle v_{y1}\rangle = 0$, and so the particles do not steadily drift off in the y direction—justifying our expansion procedure (which required that $y - y_{gc,i}$ not grow without bound) *a posteriori*. The particles do, however, steadily drift

off in the x direction, since

$$\langle v_{x1} \rangle = -\frac{\langle v_{x0}(y_0 - y_{\mathrm{gc},i}) \rangle}{B_{\mathrm{gc},i}} \frac{\mathrm{d}B}{\mathrm{d}y}. \tag{3.7}$$

Referring to equation (2.11) and taking $\delta = 0$, we arrive at

$$\begin{aligned} \langle v_{x0}(y_0 - y_{\mathrm{gc},i}) \rangle &= \pm \langle \mathrm{Re}[v_\perp \exp(\mathrm{i}\omega_\mathrm{c} t)] \, \mathrm{Re}[(v_\perp/\omega_\mathrm{c}) \exp(\mathrm{i}\omega_\mathrm{c} t)] \rangle \\ &= \pm v_\perp^2/(2\omega_\mathrm{c}) \end{aligned} \tag{3.8}$$

where the $\pm$ sign goes with the charge of the particle. Note that $\langle v_{x1} \rangle$ *does not even have a slow time derivative*, so our assumption that $\langle m\dot{v}_{x1} \rangle$ was negligible is also consistent with our solution. Note also that $B_\mathrm{gc} = B_{\mathrm{gc},i}$, because the particle is drifting in a direction in which B is constant.

Problem 3.2: Evaluate $\langle v_{x0}(y_0 - y_{\mathrm{gc},i}) \rangle$ for arbitrary δ.

Recognizing that the choices for $\mathbf{B}$ to be in the z direction and for ∇B to be in the y direction were arbitrary, we have for *perpendicular* gradients of B, a guiding-center drift given by

$$\mathbf{v}_\mathrm{grad} = \pm \frac{v_\perp^2}{2\omega_\mathrm{c}} \frac{\mathbf{B} \times \nabla B}{B^2} = \frac{W_\perp}{q} \frac{\mathbf{B} \times \nabla B}{B^3} \tag{3.9}$$

where $\mathbf{v}_\mathrm{grad}$ is the gyro-averaged drift of the guiding-center, due to a perpendicular gradient in B. We call this the '∇B drift'. In SI units, with energies in eV, equation (3.9) is particularly simple to evaluate: for a 1 000 eV particle (and all its energy in $W_\perp$), in a 1 tesla magnetic field, with a gradient scale-length of 1 meter, the ∇B drift velocity is simply 10^3 meters/second.

Note that the ∇B drift, like the gravitational drift, depends on the sign of the charge of the particle, and so it gives rise to a net current, which in turn leads to charge separation in a finite plasma and, consequently, a volumetric electric field. Interestingly, at fixed energy the ∇B drift is independent of particle mass. Notice that if $v_\perp$ is of order $v_\parallel$, this first-order gyro-averaged drift is indeed a factor kr_L smaller than the parallel velocity of the particle along a field line, $v_\parallel \hat{\mathbf{b}}$, which is the only zeroth-order motion that would survive gyro-averaging. This is consistent with our ordering procedure.

Problem 3.3: Assume $e\phi$ is of order W, a particle's kinetic energy, and that the gradient scale-length of the electric potential is roughly the same

size, $1/k$, as the scale-length of variation of B. Show that $\mathbf{v}_E$ is the same order in kr_L as $\mathbf{v}_{grad}$.

There is a simple physical picture for the ∇B drift, which follows from the fact that the local radius-of-curvature of the gyro-orbit is smaller on the larger-magnetic-field side of the orbit, and correspondingly larger on the smaller-magnetic-field side. If we construct a continuous trajectory from smaller orbits on one side, and larger orbits on the other, we find a net drift perpendicular to both $\mathbf{B}$ and ∇B, as illustrated in Figure 3.1.

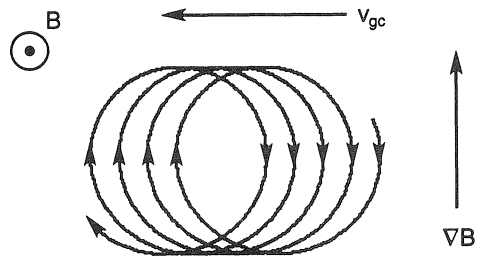

Figure 3.1. Ion ∇B drift motion. The combined effect of smaller gyro-orbits on the high-field side and larger gyro-orbits on the low-field side produces a net leftward drift of the guiding center. The dot indicates that the magnetic field faces out of the page.

3.2 CURVATURE DRIFT

In the previous Section, we made the assumption that there was a gradient in the magnetic field strength, B, but that the vector $\mathbf{B}$ was purely in the z direction, i.e. the magnetic field lines were straight. As we saw, this required volume currents, but these did not affect our analysis. Now we will make another special, but useful, simplifying assumption: that the field lines are locally curved with radius-of-curvature $\mathbf{R}_c$, but that the field strength B is locally constant. A magnetic field with these properties can also be achieved with volume currents. Imagine a current-carrying cylinder with $j_z \propto r^{-1}$ where j_z is the current density in the z direction. The total current I in the z direction within any radius r then increases linearly with r, i.e. $I \propto r$, so that from the usual formula $B \propto I/r$, the θ-directed magnetic field is independent of r. Again, these volume currents are an artifact employed to produce the assumed magnetic field; they do not enter into the analysis of particle drifts.

Now we will solve for the guiding-center drift in a locally cylindrical coordinate system (r, θ, z) matched to the local curvature of the magnetic field

lines, such that $\hat{\boldsymbol{\theta}} = \hat{\mathbf{b}}$. To zeroth order in kr_L, particles move along the θ-directed field lines with parallel velocity $v_\parallel \hat{\mathbf{b}}$, and spiral around the field lines with speed $v_\perp$. To solve for the first-order motion, we transform to the rotating frame that is moving with the zeroth-order particle motion in the θ direction. In this frame, the usual equations of motion hold, except for a centrifugal 'pseudo-force' in the radial direction, namely

$$\mathbf{F}_{cf} = \frac{mv_\parallel^2}{R_c}\hat{\mathbf{r}} = mv_\parallel^2 \frac{\mathbf{R}_c}{R_c^2} \tag{3.10}$$

where we have defined a radius-of-curvature vector $\mathbf{R}_c$ which is drawn from the local center-of-curvature to the field-line, as shown in Figure 3.2. (A Coriolis pseudo-force could also arise from drift motion in this rotating frame, but it will turn out that the drift motion is parallel to the axis of rotation, so the Coriolis force is zero in this particular case.)

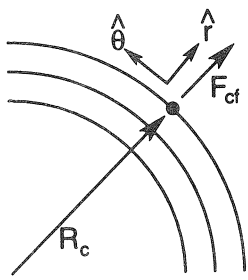

Figure 3.2. Geometry for calculating the curvature drift. The radius-of-curvature vector is drawn from the local center-of-curvature to the field line.

Using equation (2.22), we can then directly deduce

$$\mathbf{v}_{curv} = \frac{mv_\parallel^2}{qB^2}\frac{\mathbf{R}_c \times \mathbf{B}}{R_c^2} = \frac{2W_\parallel}{qB^2}\frac{\mathbf{R}_c \times \mathbf{B}}{R_c^2} \tag{3.11}$$

where $W_\parallel$ is the particle's parallel energy. The vector radius-of-curvature, $\mathbf{R}_c$, may not be a familiar way to describe local magnetic field geometry. In fact, however, any curved magnetic field can be characterized locally by a radius-of-curvature $\mathbf{R}_c$, meaning that $d\hat{\mathbf{b}}/ds$ (where s measures length along the field line) $= -\mathbf{R}_c/R_c^2$. This is easily verified for the locally cylindrical geometry we have assumed, where the equivalent statement is just $(1/r)d\hat{\boldsymbol{\theta}}/d\theta = -\hat{\mathbf{r}}/r$. Since the d/ds operator is just the derivative along the direction $\hat{\mathbf{b}}$, the radius-of-curvature can be re-expressed

$$\mathbf{R}_c/R_c^2 = -(\hat{\mathbf{b}} \cdot \nabla)\hat{\mathbf{b}} \tag{3.12}$$

giving a more common expression for the 'curvature drift'

$$\mathbf{v}_{curv} = \left(\frac{2W_\parallel}{qB^2}\right)\mathbf{B} \times [(\hat{\mathbf{b}} \cdot \nabla)\hat{\mathbf{b}}]. \tag{3.13}$$